Journal of Computational Physics **170,** 141–160 (2001)
doi:10.1006/jcph.2001.6728, available online at http://www.idealibrary.com on IDEAL®

A Solution Method of Nonlinear Convective Stability Problems in Finite Domains

H. M. Park and D. H. Ryu

Department of Chemical Engineering, Sogang University, Seoul, South Korea
E-mail: hmpark@ccs.sogang.ac.kr

Received August 25, 2000; revised December 20, 2000

A Chebyshev pseudospectral method is generalized to solve the linear and nonlinear hydrodynamic stability problems of thermal convection in a two-dimensional rectangular box with rigid sidewalls, where there may exist a heat source or a magnetic field to enhance or suppress the convection. The incompressibility condition is imposed rigorously on all boundaries. The effects of box aspect ratio, heat source, and magnetic field on the critical Rayleigh number and convection cell size are examined and compared with the results of other investigators. We have extended the present technique to nonlinear stability analysis and derived the Landau equation that describes the temporal evolution of the strength of convection in the rectangular box with rigid sidewalls. The results of nonlinear stability analysis are compared with the exact results obtained by the numerical solution of the Boussinesq equation. The present technique solves linear and nonlinear convective stability problems accurately and can be employed to solve other hydrodynamic stability problems in finite domains.

Key Words: nonlinear hydrodynamic stability; finite domain.

1. INTRODUCTION

The convective instability of Boussinesq fluids heated from below is one of the most extensively studied problems of hydrodynamic stability because of its frequent occurrence in various fields of science and engineering. A full account of the linearized theory is given in Chandrasekhar [1] and Drazin and Reid [2]. This linear theory determines the critical Rayleigh number and wavenumber but does not say anything about the magnitude of the amplitude of the convection cell finally obtained. The answer to this question is supplied by the nonlinear stability analysis based on perturbation techniques. The first work in this direction was done by Malkus and Veronis [3] and generalized by Schlüter *et al.* [4] and many others. All these analyses assume that the flow and temperature fields are periodic in the horizontal directions and seek normal mode solutions so that the resulting

0021-9991/01 $35.00

governing equations for the hydrodynamic stability become one dimensional. But these results are not comparable with experiments, since the necessary lateral confining walls render the flow pattern much more complicated, making the size of convection cells in the domain nonidentical. Davis [5] was the first investigator to consider a hydrodynamic stability problem in a finite domain where the fluid is fully confined. He studied the influence of nonslip lateral walls on the convective process in a rectangular box using a Galerkin method. Later, Reddy and Voyé [6] and van de Vooren and Dijkstra [7] employed a finite element method to analyze linear convective instability in finite domains.

In the present investigation, we employ a Chebyshev pseudospectral method [8, 9] to solve the linear and nonlinear Rayleigh–Bénard convection problems in a two-dimensional box with rigid sidewalls. The Boussinesq equation is reformulated using the stream function so that the incompressibility condition is imposed exactly. The resulting eigenvalue problem involves a biharmonic operator with two boundary conditions on each boundary, i.e., one Dirichlet condition and one Neumann condition. By judicious use of the Chebyshev pseudospectral method, these two boundary conditions are imposed on each boundary directly without introducing an auxiliary function such as vorticity. The discretized governing equation yields the eigenvalues and eigenvectors needed in the linear stability analysis. The critical eigenvalue and eigenvector are further employed in the nonlinear stability analysis, which is based on the power series method [4]. In contrast to the usual cases with periodic boundary conditions in the horizontal direction, the present problem with rigid sidewalls produces perturbation equations that cannot be solved analytically. We solve these perturbation equations numerically using the Chebyshev pseudospectral method and obtain the Landau equation after imposing the solvability condition. This technique is an extension of the semianalytic method employed in the nonlinear hydrodynamic stability analysis for the Rayleigh–Bénard convection of viscoelastic fluids with periodic boundary condition in the horizontal direction [10, 11]. The present method is quite versatile and may be employed to solve many other hydrodynamic stability problems in confined domains.

2. FORMULATION OF THE PROBLEM

We consider a Boussinesq fluid in a two-dimensional rectangular box whose bottom is maintained at a higher temperature than the top. In addition, there may exist a heat source or a magnetic field in the domain that enhances or suppresses the thermal convection (Fig. 1). We use an asterisk to denote dimensional quantities and introduce the dimensionless variables as

$$x = \frac{x^*}{d_x}, \quad y = \frac{y^*}{d_y}, \quad t = \frac{\kappa t^*}{d_y^2}, \quad \mathbf{v} = \frac{d_y \mathbf{v}^*}{\kappa},$$
$$T = \frac{T^* - T^*_{\text{cold}}}{T^*_{\text{hot}} - T^*_{\text{cold}}}, \quad P' = \frac{d_y^2 P^*}{\rho \kappa^2}, \tag{2.1}$$

where T^* is the temperature, T^*_{cold} is the temperature at the top boundary, T^*_{hot} is the temperature at the bottom boundary, t^* is the time, $\mathbf{v}^*$ is the velocity field, P^* is the pressure field, κ is the thermal diffusivity, ρ is the density, d_x is the half width of the box, and d_y is the half depth of the box. If the fluid in the box is electrically conducting, its motion in the presence of a magnetic field gives rise to a Lorentz force which acts on the fluid so that an

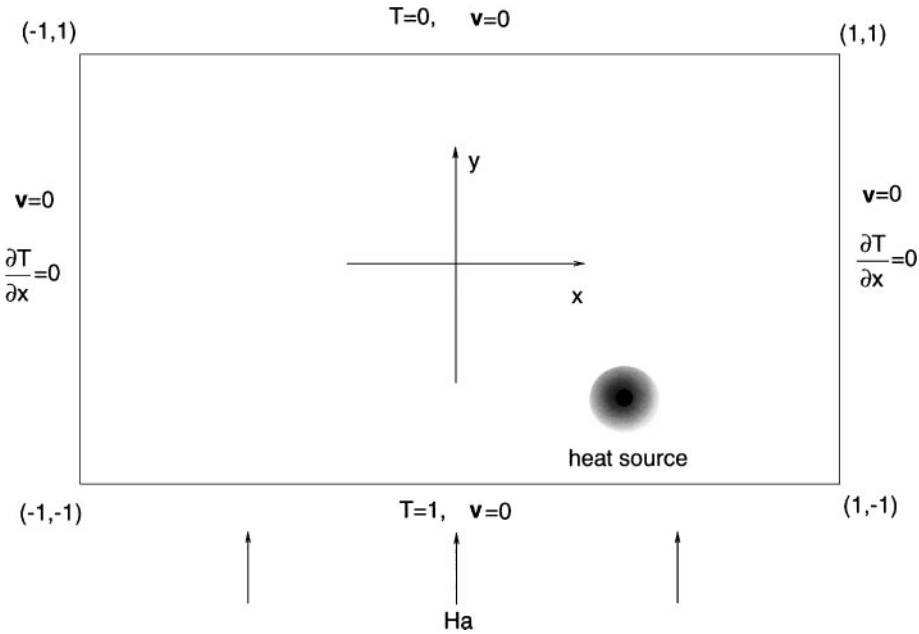

FIG. 1. The system and boundary conditions.

extra body force term appears in the Navier–Stokes equation. For most liquid metals and molten semiconductors, the magnetic Reynolds number, i.e., the ratio of magnetic induction to magnetic diffusion, is so small that the Lorentz force is practically unaffected by the flow. Further, assuming that the magnetic field is parallel to the y-axis, the Lorentz force per unit volume of fluid is given by $-\sigma_e B^2 v_x \mathbf{i}$, where σ_e is the electric conductivity of the fluid, B is the magnetic field, and v_x is the x-component of the velocity vector [12]. Thus, the set of governing equations in dimensionless variables are

$$\nabla \cdot \mathbf{v} = 0 \tag{2.2}$$

$$\frac{\partial \mathbf{v}}{\partial t} + \mathbf{v} \cdot \nabla \mathbf{v} = -\nabla P + Pr\nabla^2 \mathbf{v} + RPrT\mathbf{j} - PrHa^2 v_x \mathbf{i} \tag{2.3}$$

$$\frac{\partial T}{\partial t} + \mathbf{v} \cdot \nabla T = \nabla^2 T + G(t)\delta_n(x - x^\dagger)\delta_n(y - y^\dagger), \tag{2.4}$$

where P is the modified pressure given by

$$P = P' - (T^*_{\text{cold}} - T^*_{\text{sys}}) \frac{d_y^3}{\kappa^2} \alpha g y \tag{2.5}$$

and α is the thermal expansion coefficient. Here, T^*_{sys} is the average temperature of the system given by

$$T^*_{\text{sys}} = \frac{1}{2}(T^*_{\text{hot}} + T^*_{\text{cold}}). \tag{2.6}$$

The dimensionless group R is the Rayleigh number, Pr is the Prandtl number, and Ha is the Hartmann number defined as

$$R = \alpha g \frac{(T^*_{\text{hot}} - T^*_{\text{cold}}) d_y^3}{\kappa \nu} \tag{2.7}$$

$$Pr = \frac{\nu}{\kappa} \tag{2.8}$$

$$Ha = |B|\, dy \left(\frac{\sigma_e}{\rho \nu}\right)^{1/2}, \tag{2.9}$$

where ν is the kinematic viscosity. The dimensionless strength of heat source is denoted by $G(t)$, and the function $\delta_n(x - x^\dagger)$, which approximates the point source at $x = x^\dagger$ in the domain, is defined by

$$\delta_n(x - x^\dagger) = \frac{n}{2\cosh^2(n(x - x^\dagger))} \tag{2.10}$$

and becomes the Dirac delta function as n approaches infinity. In the present investigation, we take $n = 20$ with $(x^\dagger, y^\dagger) = (0.25, -0.25)$. The relevant boundary conditions are

$$x = \pm 1; \qquad \mathbf{v} = 0, \quad \frac{\partial T}{\partial x} = 0 \tag{2.11}$$

$$y = +1; \qquad \mathbf{v} = 0, \quad T = 0 \tag{2.12}$$

$$y = -1; \qquad \mathbf{v} = 0, \quad T = 1. \tag{2.13}$$

When the Rayleigh number R is below critical, there is no fluid motion, and the basic state or the conduction state that prevails in the system is

$$\mathbf{v} = 0 \tag{2.14}$$

$$T = \frac{1 - y}{2} + T^G(x, y), \tag{2.15}$$

where T^G satisfies the equation

$$\nabla^2 T^G + G\delta_n(x - x^\dagger)\delta_n(y - y^\dagger) = 0 \tag{2.16}$$

and the boundary conditions

$$x = \pm 1; \qquad \frac{\partial T^G}{\partial x} = 0 \tag{2.17}$$

$$y = \pm 1; \qquad T^G = 0. \tag{2.18}$$

On putting

$$T(x, y, t) = \frac{1 - y}{2} + T^G(x, y) + \Theta(x, y, t), \tag{2.19}$$

it follows that

$$\nabla \cdot \mathbf{v} = 0 \tag{2.20}$$

$$\frac{\partial \mathbf{v}}{\partial t} + \mathbf{v} \cdot \nabla \mathbf{v} = -\nabla P + Pr\nabla^2 \mathbf{v} + RPr\Theta \mathbf{j} - PrHa^2 v_x \mathbf{i} \tag{2.21}$$

$$\frac{\partial \Theta}{\partial t} + \mathbf{v} \cdot \nabla \Theta + \mathbf{v} \cdot \nabla T^G - \frac{1}{2} v_y = \nabla^2 \Theta. \tag{2.22}$$

The relevant boundary conditions are

$$x = \pm 1; \qquad \mathbf{v} = 0, \quad \frac{\partial \Theta}{\partial x} = 0 \tag{2.23}$$

$$y = \pm 1; \qquad \mathbf{v} = 0, \quad \Theta = 0. \tag{2.24}$$

In terms of the stream function Ψ, the above set of equations and boundary conditions may be rewritten as

$$\frac{\partial}{\partial t}(\nabla^2 \Psi) + J(\nabla^2 \Psi, \Psi) = Pr\nabla^4 \Psi - RPr\frac{\partial \Theta}{\partial x} - PrHa^2 \frac{\partial^2 \Psi}{\partial y^2} \tag{2.25}$$

$$\frac{\partial \Theta}{\partial t} + J(\Theta, \Psi) = \nabla^2 \Theta + \frac{\partial \Psi}{\partial x}\left(\frac{\partial T^G}{\partial y} - \frac{1}{2}\right) - \frac{\partial \Psi}{\partial y}\frac{\partial T^G}{\partial x} \tag{2.26}$$

$$x = \pm 1; \qquad \Psi = 0, \quad \frac{\partial \Psi}{\partial x} = 0, \quad \frac{\partial \Theta}{\partial x} = 0 \tag{2.27}$$

$$y = \pm 1; \qquad \Psi = 0, \quad \frac{\partial \Psi}{\partial y} = 0, \quad \Theta = 0, \tag{2.28}$$

where the Jacobian J is defined as

$$J(f, g) = \begin{vmatrix} \frac{\partial f}{\partial x} & \frac{\partial f}{\partial y} \\ \frac{\partial g}{\partial x} & \frac{\partial g}{\partial y} \end{vmatrix}. \tag{2.29}$$

3. LINEAR STABILITY ANALYSIS

We assume the time dependence for the variables Ψ and Θ as

$$\Psi = e^{st}\phi(x, y) \tag{3.1}$$

$$\Theta = e^{st}\theta(x, y) \tag{3.2}$$

and decide the stability of the system based on the signature of s. For the linear stability analysis, we substitute (3.1) and (3.2) into (2.25) and (2.26) and delete nonlinear terms to find the eigenvalue problem

$$\mathbf{A}\mathbf{x} = s\mathbf{B}\mathbf{x}, \tag{3.3}$$

where the differential operators $\mathbf{A}$ and $\mathbf{B}$ are given by

$$\mathbf{A} = \begin{bmatrix} Pr\nabla^4 - PrHa^2 \frac{\partial^2}{\partial y^2} & -RPr\frac{\partial}{\partial x} \\ J(\cdot, T^G) - \frac{1}{2}\frac{\partial}{\partial x} & \nabla^2 \end{bmatrix} \tag{3.4}$$

$$\mathbf{B} = \begin{bmatrix} \nabla^2 & 0 \\ 0 & 1 \end{bmatrix}, \tag{3.5}$$

and the eigenfunction $\mathbf{x}$ is defined as

$$\mathbf{x} = \begin{bmatrix} \phi(x, y) \\ \theta(x, y) \end{bmatrix}. \tag{3.6}$$

The boundary conditions for ϕ and θ are the same as those for Ψ and Θ. The eigenvalue problem (3.3) is discretized by the Chebyshev pseudospectral method [8, 9] after relevant boundary conditions are implemented. Using the Chebyshev pseudospectral method, we can approximate differentiations of a function by matrix multiplications. The collocation points are selected as

$$x_i = \cos\left[\frac{\pi(i-1)}{NX}\right] \quad (1 \le i \le NX+1) \tag{3.7}$$

$$y_j = \cos\left[\frac{\pi(j-1)}{NY}\right] \quad (1 \le j \le NY+1), \tag{3.8}$$

where NX and NY are the number of computational cells in the x- and the y-direction, respectively. Then the first, the second, and the fourth partial derivatives of a function $f(x, y)$, defined for $-1 \le x \le 1$ and $-1 \le y \le 1$, can be approximated by

$$\frac{\partial^q f}{\partial x^q}(x_i, y_j) = \sum_{l=1}^{NX+1} \widehat{GX}_{i,l}^{(q)} f(x_l, y_j) \tag{3.9}$$

$$\frac{\partial^q f}{\partial y^q}(x_i, y_j) = \sum_{l=1}^{NY+1} \widehat{GY}_{j,l}^{(q)} f(x_i, y_l). \tag{3.10}$$

Here the matrices $\widehat{\mathbf{GX}}^{(\mathbf{q})}$ and $\widehat{\mathbf{GY}}^{(\mathbf{q})}$ are defined as

$$\widehat{\mathbf{GX}}^{(\mathbf{q})} = \mathbf{T}^{\mathbf{x}} \mathbf{GX}^{(\mathbf{q})} \widehat{\mathbf{T}^{\mathbf{x}}} \tag{3.11}$$

$$\widehat{\mathbf{GY}}^{(\mathbf{q})} = \mathbf{T}^{\mathbf{y}} \mathbf{GY}^{(\mathbf{q})} \widehat{\mathbf{T}^{\mathbf{y}}}, \tag{3.12}$$

where

$$T_{j,k}^{x} = \cos\left[\frac{(k-1)(j-1)\pi}{NX}\right] \tag{3.13}$$

$$T_{j,k}^{y} = \cos\left[\frac{(k-1)(j-1)\pi}{NY}\right] \tag{3.14}$$

and

$$\widehat{T_{k,j}^{x}} = \frac{2}{NX} \frac{1}{C_k C_j} \cos\left[\frac{(k-1)(j-1)\pi}{NX}\right] \tag{3.15}$$

$$\widehat{T_{k,j}^{y}} = \frac{2}{NY} \frac{1}{C_k C_j} \cos\left[\frac{(k-1)(j-1)\pi}{NY}\right]. \tag{3.16}$$

The matrices $\mathbf{GX^{(q)}}$ and $\mathbf{GY^{(q)}}$ are defined as

$$GX_{i,j}^{(1)} = GY_{i,j}^{(1)} = \begin{cases} 0, & \text{if } i \geq j \text{ or } i+j \text{ is even} \\ \frac{2(j-1)}{C_i}, & \text{otherwise.} \end{cases} \tag{3.17}$$

Thus

$$\mathbf{GX^{(2)}} = \mathbf{GX^{(1)}} \cdot \mathbf{GX^{(1)}} \tag{3.18}$$

and so forth. The coefficients C_i and $\bar{C}_i$ are given as

$$\bar{C}_1 = 2, \quad \bar{C}_n = 1 \ (2 \leq n \leq NX), \quad \bar{C}_{NX+1} = 2 \tag{3.19}$$

$$C_1 = 2, \quad C_n = 1 \ (2 \leq n \leq NX+1). \tag{3.20}$$

The discretization procedure for the differential operators **A** and **B** in (3.3) consists of converting various differentiations into matrix multiplications using (3.9) and (3.10) and removing boundary grid values and outermost internal grid values of ϕ and θ in terms of the remaining internal grid values by exploiting the boundary conditions. The boundary grid values may be represented in terms of internal grid values as follows. The boundary conditions

$$x = \pm 1; \qquad \phi = 0 \quad \text{and} \quad \frac{\partial \phi}{\partial x} = 0 \tag{3.21}$$

yield

$$\phi_{1,j} = 0; \quad \phi_{NX+1,j} = 0 \quad (1 \leq j \leq NY+1) \tag{3.22}$$

$$\sum_{m=1}^{NX+1} \widehat{GX}_{1,m}^{(1)} \phi_{m,j} = 0; \quad \sum_{m=1}^{NX+1} \widehat{GX}_{NX+1,m}^{(1)} \phi_{m,j} = 0 \quad (1 \leq j \leq NY+1). \tag{3.23}$$

Solving (3.22) and (3.23) simultaneously, we can express the outermost internal grid values in terms of the remaining internal grid values,

$$\phi_{2,j} = \sum_{m=3}^{NX-1} a_m \phi_{m,j}; \ \phi_{NX,j} = \sum_{m=3}^{NX-1} b_m \phi_{m,j} \quad (1 \leq j \leq NY+1), \tag{3.24}$$

where

$$a_m \equiv \frac{\widehat{GX}_{1,NX}^{(1)} \widehat{GX}_{NX+1,m}^{(1)} - \widehat{GX}_{NX+1,NX}^{(1)} \widehat{GX}_{1,m}^{(1)}}{\widehat{GX}_{1,2}^{(1)} \widehat{GX}_{NX+1,NX}^{(1)} - \widehat{GX}_{1,NX}^{(1)} \widehat{GX}_{NX+1,2}^{(1)}} \tag{3.25}$$

$$b_m \equiv \frac{\widehat{GX}_{NX+1,2}^{(1)} \widehat{GX}_{1,m}^{(1)} - \widehat{GX}_{1,2}^{(1)} \widehat{GX}_{NX+1,m}^{(1)}}{\widehat{GX}_{1,2}^{(1)} \widehat{GX}_{NX+1,NX}^{(1)} - \widehat{GX}_{1,NX}^{(1)} \widehat{GX}_{NX+1,2}^{(1)}}. \tag{3.26}$$

Similarly, the boundary conditions

$$y = \pm 1; \qquad \phi = 0 \quad \text{and} \quad \frac{\partial \phi}{\partial y} = 0 \tag{3.27}$$

yield

$$\phi_{i,1} = 0; \quad \phi_{i,NY+1} = 0 \quad (1 \le i \le NX + 1) \tag{3.28}$$

and

$$\phi_{i,2} = \sum_{l=3}^{NY-1} c_l \phi_{i,l}; \quad \phi_{i,NY} = \sum_{l=3}^{NY-1} d_l \phi_{i,l} \quad (1 \le i \le NX + 1), \tag{3.29}$$

where

$$c_l \equiv \frac{\widehat{GY}^{(1)}_{1,NY}\widehat{GY}^{(1)}_{NY+1,l} - \widehat{GY}^{(1)}_{NY+1,NY}\widehat{GY}^{(1)}_{1,l}}{\widehat{GY}^{(1)}_{1,2}\widehat{GY}^{(1)}_{NY+1,NY} - \widehat{GY}^{(1)}_{1,NY}\widehat{GY}^{(1)}_{NY+1,2}} \tag{3.30}$$

$$d_l \equiv \frac{\widehat{GY}^{(1)}_{NY+1,2}\widehat{GY}^{(1)}_{1,l} - \widehat{GY}^{(1)}_{1,2}\widehat{GY}^{(1)}_{NY+1,l}}{\widehat{GY}^{(1)}_{1,2}\widehat{GY}^{(1)}_{NY+1,NY} - \widehat{GY}^{(1)}_{1,NY}\widehat{GY}^{(1)}_{NY+1,2}}. \tag{3.31}$$

In contrast to $\phi(x, y)$, $\theta(x, y)$ has only one boundary condition at each boundary:

$$x = \pm 1; \qquad \frac{\partial \theta}{\partial x} = 0 \tag{3.32}$$

$$y = \pm 1; \qquad \theta = 0. \tag{3.33}$$

Thus, we remove only the boundary grid values of θ as follows:

$$\theta_{i,1} = 0; \quad \theta_{i,NY+1} = 0 \quad (1 \le i \le NX + 1) \tag{3.34}$$

$$\theta_{1,j} = \sum_{m=2}^{NX} a^T_m \theta_{m,j}; \quad \theta_{NX+1,j} = \sum_{m=2}^{NX} b^T_m \theta_{m,j} \quad (1 \le j \le NY + 1), \tag{3.35}$$

where

$$a^T_m \equiv \frac{\widehat{GX}^{(1)}_{1,NX+1}\widehat{GX}^{(1)}_{NX+1,m} - \widehat{GX}^{(1)}_{1,m}\widehat{GX}^{(1)}_{NX+1,NX+1}}{\widehat{GX}^{(1)}_{1,1}\widehat{GX}^{(1)}_{NX+1,NX+1} - \widehat{GX}^{(1)}_{1,NX+1}\widehat{GX}^{(1)}_{NX+1,1}} \tag{3.36}$$

$$b^T_m \equiv \frac{\widehat{GX}^{(1)}_{1,m}\widehat{GX}^{(1)}_{NX+1,1} - \widehat{GX}^{(1)}_{1,1}\widehat{GX}^{(1)}_{NX+1,m}}{\widehat{GX}^{(1)}_{1,1}\widehat{GX}^{(1)}_{NX+1,NX+1} - \widehat{GX}^{(1)}_{1,NX+1}\widehat{GX}^{(1)}_{NX+1,1}}. \tag{3.37}$$

Removing the boundary grid points and outermost internal grid points of ϕ and the boundary grid points of θ, the linearized stability equation (3.3) may be rewritten as

$$s\Bigg[\sum_{m=3}^{NX-1}\left(\widehat{GX}^{(2)}_{i,2}a_m + \widehat{GX}^{(2)}_{i,m} + \widehat{GX}^{(2)}_{i,NX}b_m\right)\phi_{m,j} + \sum_{l=3}^{NY-1}\left(\widehat{GY}^{(2)}_{j,2}c_l + \widehat{GY}^{(2)}_{j,l} + \widehat{GY}^{(2)}_{j,NY}d_l\right)\phi_{i,l}\Bigg]$$

$$
\begin{aligned}
&= Pr\Bigg[\sum_{m=3}^{NX-1}\Big(\widehat{GX}^{(4)}_{i,2}a_m + \widehat{GX}^{(4)}_{i,m} + \widehat{GX}^{(4)}_{i,NX}b_m\Big)\phi_{m,j} \\
&\quad + \sum_{l=3}^{NY-1}\Big(\widehat{GY}^{(4)}_{j,2}c_l + \widehat{GY}^{(4)}_{j,l} + \widehat{GY}^{(4)}_{j,NY}\,d_l\Big)\phi_{i,l} \\
&\quad + 2\sum_{m=3}^{NX-1}\sum_{l=3}^{NY-1}\Big\{\Big(\widehat{GX}^{(2)}_{i,2}\widehat{GY}^{(2)}_{j,2}c_l + \widehat{GX}^{(2)}_{i,2}\widehat{GY}^{(2)}_{j,l} + \widehat{GX}^{(2)}_{i,2}\widehat{GY}^{(2)}_{j,NY}\,d_l\Big)a_m \\
&\quad + \Big(\widehat{GY}^{(2)}_{j,2}\widehat{GX}^{(2)}_{i,m}\Big)c_l + \widehat{GX}^{(2)}_{i,m}\widehat{GY}^{(2)}_{j,l} + \Big(\widehat{GY}^{(2)}_{j,NY}\widehat{GX}^{(2)}_{i,m}\Big)d_l \\
&\quad + \Big(\widehat{GX}^{(2)}_{i,NX}\widehat{GY}^{(2)}_{j,2}c_l + \widehat{GX}^{(2)}_{i,NX}\widehat{GY}^{(2)}_{j,l} + \widehat{GX}^{(2)}_{i,NX}\widehat{GY}^{(2)}_{j,NY}\,d_l\Big)b_m\Big\}\phi_{m,l}\Bigg] \\
&\quad - RPr\sum_{m=2}^{NX}\Big(\widehat{GX}^{(1)}_{i,1}a^T_m + \widehat{GX}^{(1)}_{i,m} + \widehat{GX}^{(1)}_{i,NX+1}b^T_m\Big)\theta_{m,j} \\
&\quad - PrHa^2\sum_{l=3}^{NY-1}\Big(\widehat{GY}^{(2)}_{j,2}c_l + \widehat{GY}^{(2)}_{j,l} + \widehat{GY}^{(2)}_{j,NY}\,d_l\Big)\phi_{i,l}
\end{aligned}
\tag{3.38}
$$

$$
\begin{aligned}
s\theta_{ij} &= -\left(\frac{\partial T^G}{\partial x}\right)_{i,j}\sum_{l=3}^{NY-1}\Big(\widehat{GY}^{(1)}_{j,2}c_l + \widehat{GY}^{(1)}_{j,l} + \widehat{GY}^{(1)}_{j,NY}d_l\Big)\phi_{i,l} \\
&\quad + \left(\frac{\partial T^G}{\partial y} - \frac{1}{2}\right)_{i,j}\sum_{m=3}^{NX-1}\Big(\widehat{GX}^{(1)}_{i,2}a_m + \widehat{GX}^{(1)}_{i,m} + \widehat{GX}^{(1)}_{i,NX}b_m\Big)\phi_{m,j} \\
&\quad + \sum_{m=2}^{NX}\Big(\widehat{GX}^{(2)}_{i,1}a^T_m + \widehat{GX}^{(2)}_{i,m} + \widehat{GX}^{(2)}_{i,NX+1}b^T_m\Big)\theta_{m,j} + \sum_{l=2}^{NY}\widehat{GY}^{(2)}_{j,l}\theta_{i,l}.
\end{aligned}
\tag{3.39}
$$

That is, the differential eigenvalue problem (3.3) is converted into the matrix eigenvalue problem

$$\boldsymbol{\alpha}\cdot\mathbf{x} = s\boldsymbol{\beta}\cdot\mathbf{x}, \tag{3.40}$$

where the eigenvector $\mathbf{x}$ is defined as

$$\mathbf{x} = (\phi_{3,3}, \phi_{4,3}, \ldots, \phi_{NX-1,NY-1}, \theta_{2,2}, \theta_{3,2}, \ldots, \theta_{NX,NY})^T. \tag{3.41}$$

The eigenvalue s of (3.40) determines the linear stability of the basic state. The basic state becomes unstable and convective flow sets in when the real part of s becomes positive. The critical Rayleigh number is defined as the smallest Rayleigh number when the largest real part of s is zero. For Rayleigh– Bénard convection, when the largest real part of s is zero, the corresponding imaginary part of s is always zero; i.e., the exchange of stabilities is valid. When $Ha = 0$ and $T^G = 0$, i.e., for the case without a magnetic field or heat source, this is confirmed by noting that the operator $\mathbf{A}$ in (3.4) is self-adjoint. When there is a magnetic field or a heat source, the validity of the exchange of stabilities is confirmed numerically. Results are obtained for rectangular boxes having d_x/d_y ratio (aspect ratio) in the range

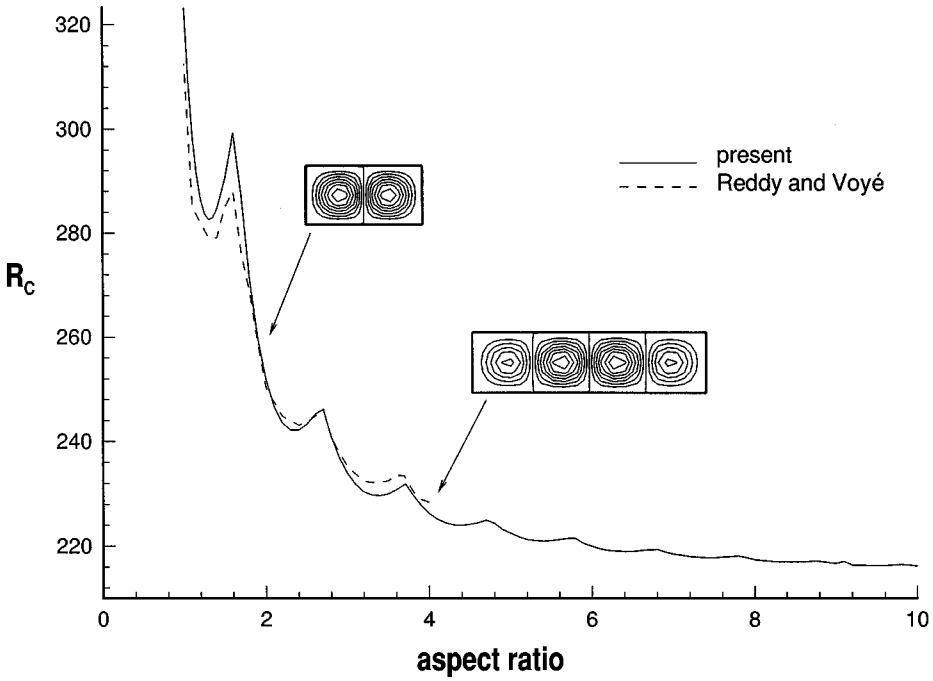

FIG. 2. Critical Rayleigh number versus the aspect ratio.

1–10 by solving the matrix eigenvalue problem (3.40) using a standard package such as IMSL. We adopt a (30×10) grid system for boxes with $1 \leq d_x/d_y \leq 3$, a (40×10) grid for $3 \leq d_x/d_y \leq 7$, and a (50×10) grid for $7 \leq d_x/d_y \leq 10$ with double precision arithmetic. The use of finer meshes does not change the results. Figure 2 shows the critical Rayleigh number for the aspect ratio in the range 1–10. The result obtained by Reddy and Voyé [6] is presented in the figure for comparison. Both results show that the envelope of least eigenvalues is a piecewise smooth curve, each smooth section of the curve corresponding to a particular mode number, i.e., number of convection cells at onset of instability. The mode number increases discretely as the aspect ratio d_x/d_y increases. The most dangerous modes at certain aspect ratios are also plotted in the figure.

Next, we investigate the effect of the heat source on the critical Rayleigh number. Figure 3 presents the variation of the critical Rayleigh number versus the strength of a heat source located at $(0.25, -0.25)$ when the box aspect ratio d_x/d_y is 2. When the heat source is located at this position, the increased strength of the heat source (positive G) destabilizes the system and, consequently, reduces the critical Rayleigh number. A negative value of G denotes the presence of a heat sink at the same location. Figure 3 also shows that the presence of a heat sink at this location $(0.25, -0.25)$ stabilizes the system until G becomes approximately -6. Any further decrease of G, i.e., increase in the strength of the heat sink, destabilizes the system and decreases the critical Rayleigh number. The most dangerous modes, i.e., the eigenfunction with zero eigenvalue at the critical Rayleigh number, for several values of G are also plotted in Fig. 3.

Figure 4 shows the effect of the location of a heat source of strength $G = 1.0$ on the critical Rayleigh number. The critical Rayleigh numbers are shown as contours for various locations of the heat source. A heat source located in the lower half of the domain destabilizes the fluid motion, while a heat source in the upper half of the domain stabilizes the system. At

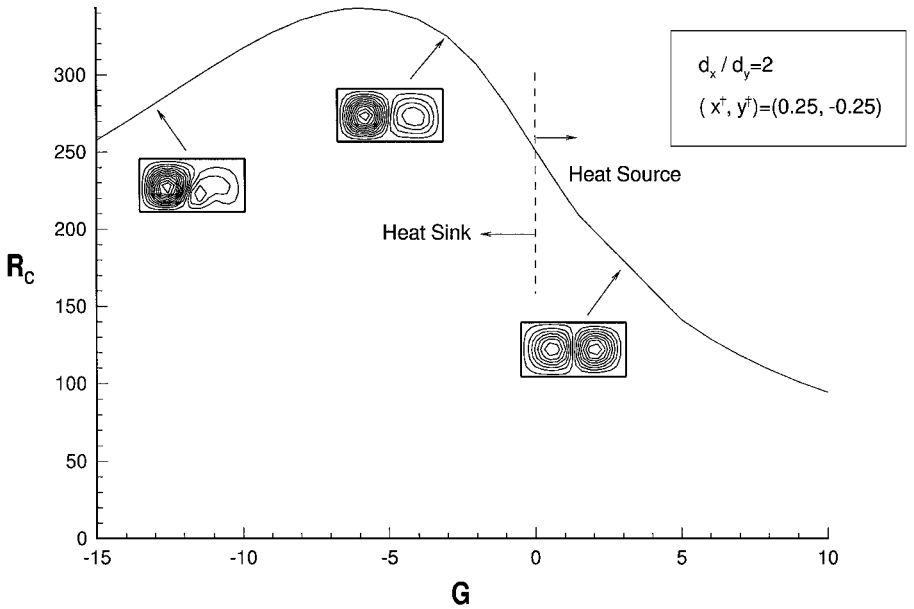

FIG. 3. Effect of the strength of heat source at (0.25, −0.25) on the critical Rayleigh number when the aspect ratio is 2.

the same vertical location, the destabilizing effect of the heat source increases as its location moves toward the sidewalls for the upper half domain, while the trend is reversed in the lower half domain. In Figs. 5a–5d are shown the velocity and temperature eigenfunctions at the critical Rayleigh number when a heat source of strength $G = 1.0$ is located at (0.5, 0.5) and (−0.5, 0.5), respectively.

Figure 6 plots the effect of the Hartmann number on the critical Rayleigh number for Boussinesq fluids with electric conductivity, such as liquid metals or semiconductor

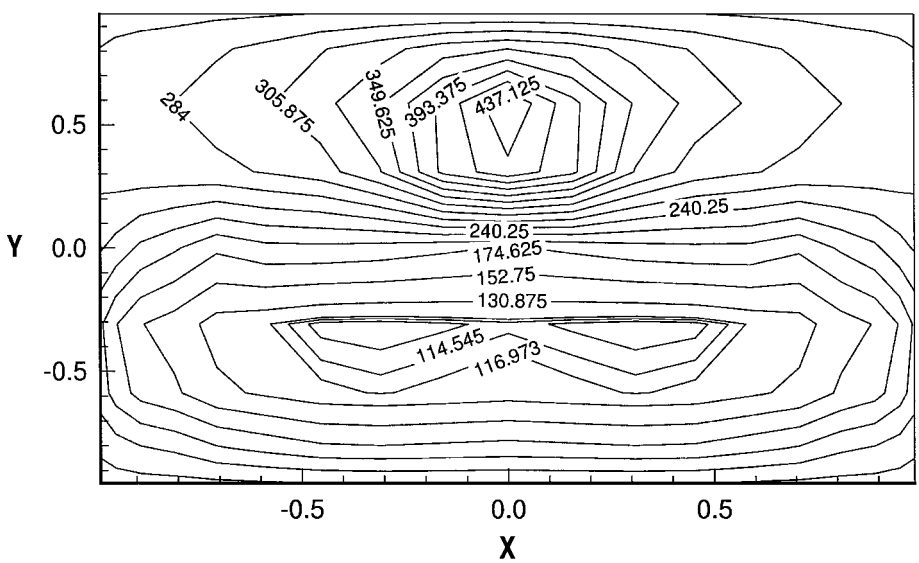

FIG. 4. Effect of the location of heat source on the critical Rayleigh number ($d_x/d_y = 2$; $G = 1$).

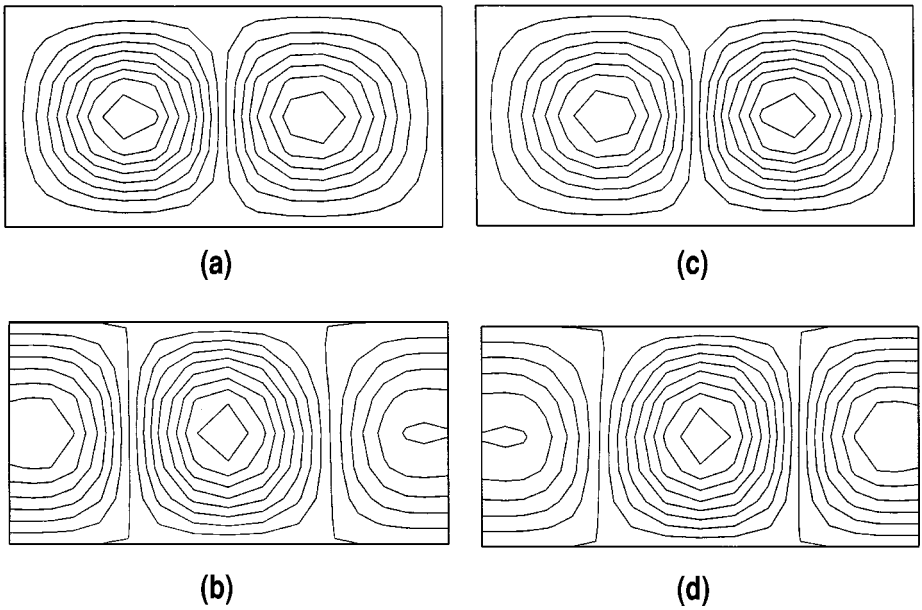

FIG. 5. The velocity and temperature eigenfunctions at the critical Rayleigh number when a heat source is present: (a) velocity eigenfunction when $(x^{\dagger}, y^{\dagger}) = (0.5, 0.5)$, (b) temperature eigenfunction when $(x^{\dagger}, y^{\dagger}) = (0.5, 0.5)$, (c) velocity eigenfunction when $(x^{\dagger}, y^{\dagger}) = (-0.5, 0.5)$, and (d) temperature eigenfunction when $(x^{\dagger}, y^{\dagger}) = (-0.5, 0.5)$.

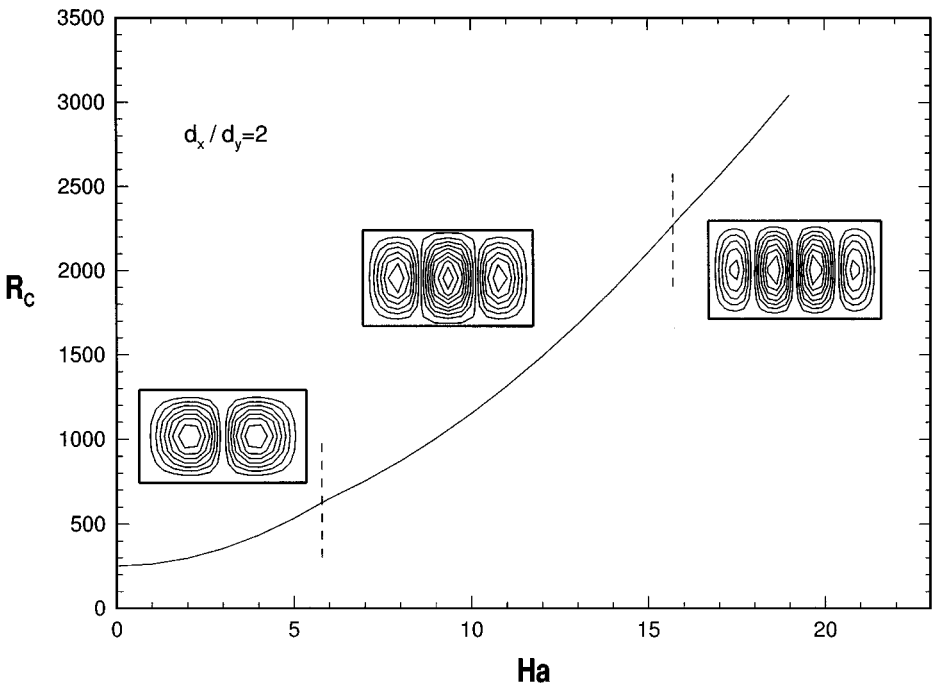

FIG. 6. Effect of magnetic field on the critical Rayleigh number.

materials. It is shown that the critical Rayleigh number increases as the strength of the magnetic field increases. It is also shown that as the Hartmann number increases, the mode number (wavenumber) increases. The Hartmann number boundaries where the mode number changes are indicated by dashed lines, when $d_x/d_y = 2$.

4. NONLINEAR STABILITY ANALYSIS

The linear stability analysis gives the critical Rayleigh number, but does not predict the magnitude of the convection cell. In this section we employ the power series method [4, 10, 11] to obtain an explicit expression for the magnitude of convection cell near the critical Rayleigh number. For brevity of analysis, we consider only the case with $G = 0$ and $Ha = 0$. Extension of the present analysis to the cases of nonzero G and Ha is trivial. Introducing a small perturbation parameter ϵ, which indicates deviation from the critical state, the variables may be expanded as power series of ϵ for a weak nonlinear state:

$$R = R_c + \epsilon^2 R_2 + \cdots \tag{4.1}$$

$$\Theta = \epsilon\Theta_1 + \epsilon^2\Theta_2 + \epsilon^3\Theta_3 + \cdots \tag{4.2}$$

$$\Psi = \epsilon\Psi_1 + \epsilon^2\Psi_2 + \epsilon^3\Psi_3 + \cdots. \tag{4.3}$$

The scaling for the time variable t is such that $\partial/\partial t = \epsilon^2\partial/\partial\tau$. The term R_1 in (4.1) is eliminated a priori, since it becomes zero due to the symmetry when the solvability condition is imposed. When the disturbance variables defined as above are substituted into the governing equation, we find the following sequence of equations:

$O(\epsilon)$

$$Pr\nabla^4\Psi_1 - R_c Pr\frac{\partial\Theta_1}{\partial x} = 0 \tag{4.4}$$

$$\nabla^2\Theta_1 - \frac{1}{2}\frac{\partial\Psi_1}{\partial x} = 0 \tag{4.5}$$

$O(\epsilon^2)$

$$Pr\nabla^4\Psi_2 - R_c Pr\frac{\partial\Theta_2}{\partial x} = \frac{\partial\nabla^2\Psi_1}{\partial x}\frac{\partial\Psi_1}{\partial y} - \frac{\partial\nabla^2\Psi_1}{\partial y}\frac{\partial\Psi_1}{\partial x} \tag{4.6}$$

$$\nabla^2\Theta_2 - \frac{1}{2}\frac{\partial\Psi_2}{\partial x} = \frac{\partial\Theta_1}{\partial x}\frac{\partial\Psi_1}{\partial y} - \frac{\partial\Theta_1}{\partial y}\frac{\partial\Psi_1}{\partial x} \tag{4.7}$$

$O(\epsilon^3)$

$$\begin{aligned} Pr\nabla^4\Psi_3 - R_c Pr\frac{\partial\Theta_3}{\partial x} = {} & \frac{\partial}{\partial\tau}\nabla^2\Psi_1 + \frac{\partial\nabla^2\Psi_1}{\partial x}\frac{\partial\Psi_2}{\partial y} + \frac{\partial\nabla^2\Psi_2}{\partial x}\frac{\partial\Psi_1}{\partial y} - \frac{\partial\nabla^2\Psi_1}{\partial y}\frac{\partial\Psi_2}{\partial x} \\ & - \frac{\partial\nabla^2\Psi_2}{\partial y}\frac{\partial\Psi_1}{\partial x} + R_2 Pr\frac{\partial\Theta_1}{\partial x} \end{aligned} \tag{4.8}$$

$$\nabla^2\Theta_3 - \frac{1}{2}\frac{\partial\Psi_3}{\partial x} = \frac{\partial\Theta_1}{\partial\tau} + \frac{\partial\Theta_1}{\partial x}\frac{\partial\Psi_2}{\partial y} + \frac{\partial\Theta_2}{\partial x}\frac{\partial\Psi_1}{\partial y} - \frac{\partial\Theta_1}{\partial y}\frac{\partial\Psi_2}{\partial x} - \frac{\partial\Theta_2}{\partial y}\frac{\partial\Psi_1}{\partial x}. \tag{4.9}$$

The relevant boundary conditions are

$$x = \pm 1; \qquad \Psi_i = 0, \quad \frac{\partial \Psi_i}{\partial x} = 0, \quad \frac{\partial \Theta_i}{\partial x} = 0 \quad (i = 1, 2, 3) \tag{4.10}$$

$$y = \pm 1; \qquad \Psi_i = 0, \quad \frac{\partial \Psi_i}{\partial y} = 0, \quad \Theta_i = 0 \quad (i = 1, 2, 3). \tag{4.11}$$

The perturbation equation for each order i may be solved as follows.

(1) First order (ϵ). The first-order equations, Eqs. (4.4) and (4.5), with the relevant boundary conditions are the same as those for the linear stability analysis, Eq. (3.3), with $s = 0$. Therefore, Eqs. (4.4) and (4.5) may be discretized as

$$\boldsymbol{\alpha} \cdot \mathbf{x}_{(1)} = 0. \tag{4.12}$$

Here $\boldsymbol{\alpha}$ is the same matrix as defined in Eq. (3.40) and $\mathbf{x}_{(1)}$ is defined as

$$\mathbf{x}_{(1)} = \left(\Psi^{(1)}_{3,3}, \Psi^{(1)}_{4,3}, \ldots, \Psi^{(1)}_{NX-1,NY-1}, \Theta^{(1)}_{2,2}, \Theta^{(1)}_{3,2}, \ldots, \Theta^{(1)}_{NX,NY} \right)^T. \tag{4.13}$$

The solution of Eq. (4.12) is the eigenvector $\mathbf{x}$ of the linear stability equation (Eq. (3.40)) with zero eigenvalue ($s = 0$). We may write the first-order solution as

$$\mathbf{x}_{(1)} = C\mathbf{x}, \tag{4.14}$$

where $\mathbf{x}$ is given by Eq. (3.41). Here the amplitude $C = C(\tau)$ is introduced since the magnitude of an eigenvector is arbitrary. The amplitude C is determined during the solution process for the third-order equations.

(2) Second order (ϵ^2). Since the differential operator defining the left-hand side of the second-order equations, Eqs. (4.6) and (4.7), is the same as that for the linear stability analysis, Eq. (3.4), with $T^G = 0$ and $Ha = 0$, we may write the discretized form of the second-order equations as

$$\boldsymbol{\alpha} \cdot \mathbf{x}_{(2)} \; = \; \mathbf{f}_{(2)}. \tag{4.15}$$

Here $\boldsymbol{\alpha}$ is the same matrix as defined in Eq. (3.40) and $\mathbf{x}_{(2)}$ is given by

$$\mathbf{x}_{(2)} \; = \; \left(\Psi^{(2)}_{3,3}, \Psi^{(2)}_{4,3}, \ldots, \Psi^{(2)}_{NX-1,NY-1}, \Theta^{(2)}_{2,2}, \Theta^{(2)}_{3,2}, \ldots, \Theta^{(2)}_{NX,NY} \right)^T. \tag{4.16}$$

The right-hand side of Eq. (4.15) is given by

$$\mathbf{f}_{(2)} = \begin{bmatrix} \left(\frac{\partial \nabla^2 \Psi_1}{\partial x} \frac{\partial \Psi_1}{\partial y} - \frac{\partial \nabla^2 \Psi_1}{\partial y} \frac{\partial \Psi_1}{\partial x} \right)_{3,3} \\ \vdots \\ \left(\frac{\partial \nabla^2 \Psi_1}{\partial x} \frac{\partial \Psi_1}{\partial y} - \frac{\partial \nabla^2 \Psi_1}{\partial y} \frac{\partial \Psi_1}{\partial x} \right)_{NX-1,NY-1} \\ \left(\frac{\partial \Theta_1}{\partial x} \frac{\partial \Psi_1}{\partial y} - \frac{\partial \Theta_1}{\partial y} \frac{\partial \Psi_1}{\partial x} \right)_{2,2} \\ \vdots \\ \left(\frac{\partial \Theta_1}{\partial x} \frac{\partial \Psi_1}{\partial y} - \frac{\partial \Theta_1}{\partial y} \frac{\partial \Psi_1}{\partial x} \right)_{NX,NY} \end{bmatrix} = C^2 \begin{bmatrix} \left(\frac{\partial \nabla^2 \phi}{\partial x} \frac{\partial \phi}{\partial y} - \frac{\partial \nabla^2 \phi}{\partial y} \frac{\partial \phi}{\partial x} \right)_{3,3} \\ \vdots \\ \left(\frac{\partial \nabla^2 \phi}{\partial x} \frac{\partial \phi}{\partial y} - \frac{\partial \nabla^2 \phi}{\partial y} \frac{\partial \phi}{\partial x} \right)_{NX-1,NY-1} \\ \left(\frac{\partial \theta}{\partial x} \frac{\partial \phi}{\partial y} - \frac{\partial \theta}{\partial y} \frac{\partial \phi}{\partial x} \right)_{2,2} \\ \vdots \\ \left(\frac{\partial \theta}{\partial x} \frac{\partial \phi}{\partial y} - \frac{\partial \theta}{\partial y} \frac{\partial \phi}{\partial x} \right)_{NX,NY} \end{bmatrix}. \tag{4.17}$$

Equation (4.15) can be easily solved to yield $\mathbf{x}_{(2)}$.

(3) Third order (ϵ^3). The differential operator for the left-hand side of the third-order equations, Eqs. (4.8) and (4.9), is also identical to that for the linear stability analysis, Eq. (3.4), with $Ha = 0$ and $T^G = 0$. Therefore, we may discretize the third-order equations as

$$\boldsymbol{\alpha} \cdot \mathbf{x}_{(3)} = \frac{\partial}{\partial \tau}\mathbf{f}^{(3)} + R_2 Pr \mathbf{g}^{(3)} + \mathbf{h}^{(3)}, \tag{4.18}$$

where $\boldsymbol{\alpha}$ is the same matrix as defined in Eq. (3.40), and $\mathbf{x}_{(3)}$ is given by

$$\mathbf{x}_{(3)} = \left(\Psi^{(3)}_{3,3}, \Psi^{(3)}_{4,3}, \ldots, \Psi^{(3)}_{NX-1,NY-1}, \Theta^{(3)}_{2,2}, \Theta^{(3)}_{3,2}, \ldots, \Theta^{(3)}_{NX,NY}\right)^T. \tag{4.19}$$

The vectors $\mathbf{f}^{(3)}$, $\mathbf{g}^{(3)}$, and $\mathbf{h}^{(3)}$ are defined as

$$\mathbf{f}^{(3)} = \begin{bmatrix} (\nabla^2\Psi_1)_{3,3} \\ \vdots \\ (\nabla^2\Psi_1)_{NX-1,NY-1} \\ (\Theta_1)_{2,2} \\ \vdots \\ (\Theta_1)_{NX,NY} \end{bmatrix} = C \begin{bmatrix} (\nabla^2\phi)_{3,3} \\ \vdots \\ (\nabla^2\phi)_{NX-1,NY-1} \\ (\theta)_{2,2} \\ \vdots \\ (\theta)_{NX,NY} \end{bmatrix} = C\mathbf{F}^{(3)} \tag{4.20}$$

$$\mathbf{g}^{(3)} = \begin{bmatrix} \left(\frac{\partial\Theta_1}{\partial x}\right)_{3,3} \\ \vdots \\ \left(\frac{\partial\Theta_1}{\partial x}\right)_{NX-1,NY-1} \\ 0 \\ 0 \\ \vdots \\ 0 \end{bmatrix} = C \begin{bmatrix} \left(\frac{\partial\theta}{\partial x}\right)_{3,3} \\ \vdots \\ \left(\frac{\partial\theta}{\partial x}\right)_{NX-1,NY-1} \\ 0 \\ 0 \\ \vdots \\ 0 \end{bmatrix} = C\mathbf{G}^{(3)} \tag{4.21}$$

$$\mathbf{h}^{(3)} = \begin{bmatrix} \left(\frac{\partial\nabla^2\Psi_1}{\partial x}\frac{\partial\Psi_2}{\partial y} + \frac{\partial\nabla^2\Psi_2}{\partial x}\frac{\partial\Psi_1}{\partial y} - \frac{\partial\nabla^2\Psi_1}{\partial y}\frac{\partial\Psi_2}{\partial x} - \frac{\partial\nabla^2\Psi_2}{\partial y}\frac{\partial\Psi_1}{\partial x}\right)_{3,3} \\ \vdots \\ \left(\frac{\partial\nabla^2\Psi_1}{\partial x}\frac{\partial\Psi_2}{\partial y} + \frac{\partial\nabla^2\Psi_2}{\partial x}\frac{\partial\Psi_1}{\partial y} - \frac{\partial\nabla^2\Psi_1}{\partial y}\frac{\partial\Psi_2}{\partial x} - \frac{\partial\nabla^2\Psi_2}{\partial y}\frac{\partial\Psi_1}{\partial x}\right)_{NX-1,NY-1} \\ \left(\frac{\partial\Theta_1}{\partial x}\frac{\partial\Psi_2}{\partial y} + \frac{\partial\Theta_2}{\partial x}\frac{\partial\Psi_1}{\partial y} - \frac{\partial\Theta_1}{\partial y}\frac{\partial\Psi_2}{\partial x} - \frac{\partial\Theta_2}{\partial y}\frac{\partial\Psi_1}{\partial x}\right)_{2,2} \\ \vdots \\ \left(\frac{\partial\Theta_1}{\partial x}\frac{\partial\Psi_2}{\partial y} + \frac{\partial\Theta_2}{\partial x}\frac{\partial\Psi_1}{\partial y} - \frac{\partial\Theta_1}{\partial y}\frac{\partial\Psi_2}{\partial x} - \frac{\partial\Theta_2}{\partial y}\frac{\partial\Psi_1}{\partial x}\right)_{NX,NY} \end{bmatrix} = C^3\mathbf{H}^{(3)}. \tag{4.22}$$

Since the vector $\mathbf{h}^{(3)}$ consists of terms which are multiples of the first-order solution and the second-order solution, it is proportional to C^3.

(4) Adjoint problem. The adjoint equation to the linear stability problem, Eq. (3.40), is given by

$$(\boldsymbol{\beta}^{-1} \cdot \boldsymbol{\alpha})^T \cdot \mathbf{y} = -s\mathbf{y}, \tag{4.23}$$

where the superscript T denotes the matrix transpose. The eigenvector $\mathbf{y}$ with zero eigenvalue ($s = 0$) is the adjoint solution of the linear stability problem. Now we are in a position to derive the Landau equation that describes the temporal variation of the amplitude C of the convection cell. Multiplying both sides of Eq. (4.18) by $\boldsymbol{\beta}^{-1}$, where $\boldsymbol{\beta}$ is defined in

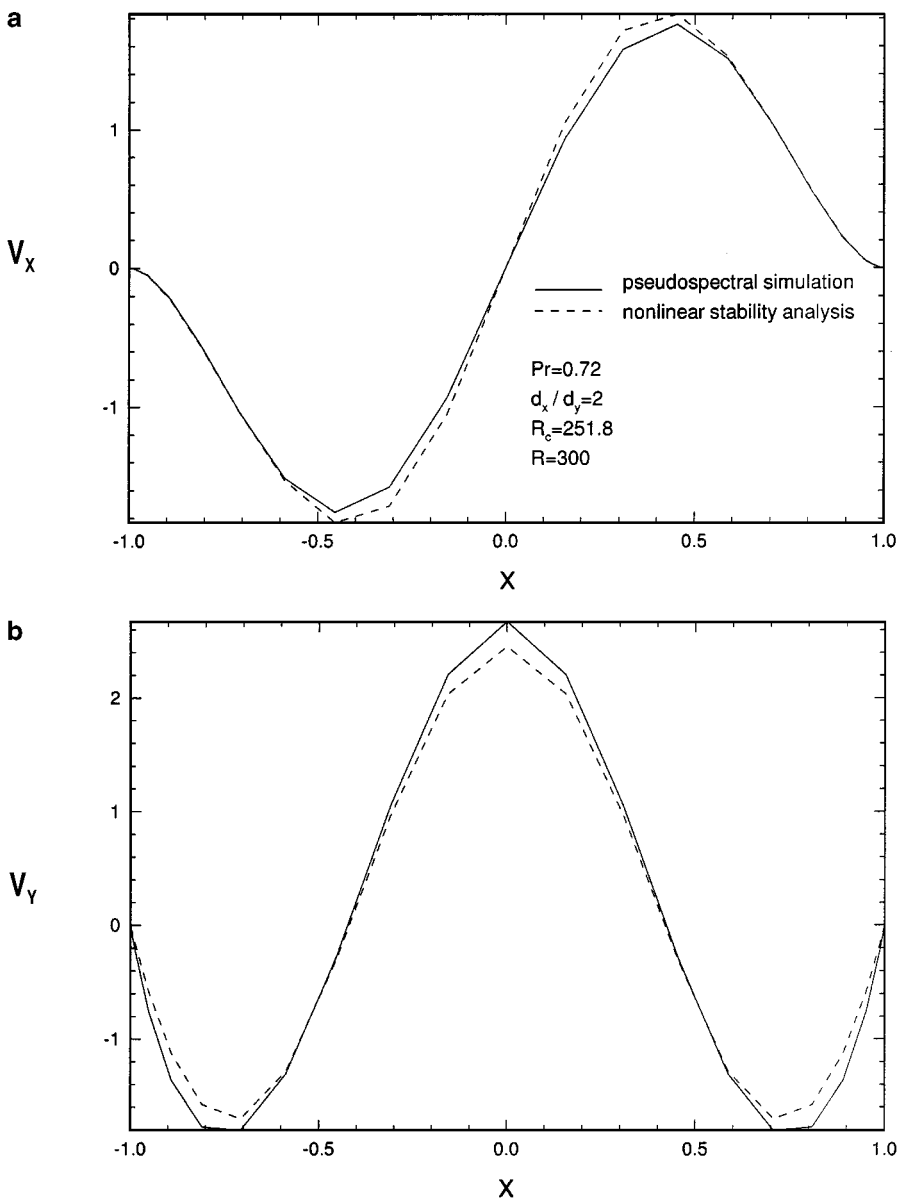

FIG. 7. Velocity components obtained by the nonlinear stability analysis and pseudospectral simulation when $d_x/d_y = 2$: (a) v_x, (b) v_y.

Eq. (3.40), and taking inner product of the resulting equation with the adjoint vector **y** (cf. Eq. (4.23)), we find

$$\left\langle \mathbf{y}, (\boldsymbol{\beta}^{-1}\cdot\boldsymbol{\alpha})\cdot\mathbf{x}_{(3)}\right\rangle = \frac{\partial}{\partial\tau}\left\langle \mathbf{y}, \boldsymbol{\beta}^{-1}\cdot\mathbf{f}^{(3)}\right\rangle + R_2 Pr\left\langle \mathbf{y}, \boldsymbol{\beta}^{-1}\cdot\mathbf{g}^{(3)}\right\rangle + \left\langle \mathbf{y}, \boldsymbol{\beta}^{-1}\cdot\mathbf{h}^{(3)}\right\rangle. \quad (4.24)$$

Since the left-hand side of Eq. (4.24) is zero from the definition of the adjoint solution, we find the following form of the Landau equation:

$$\left\langle \mathbf{y}, \boldsymbol{\beta}^{-1}\cdot\mathbf{F}^{(3)}\right\rangle \frac{\partial C}{\partial\tau} + R_2 PrC\left\langle \mathbf{y}, \boldsymbol{\beta}^{-1}\cdot\mathbf{G}^{(3)}\right\rangle + C^3\left\langle \mathbf{y}, \boldsymbol{\beta}^{-1}\cdot\mathbf{H}^{(3)}\right\rangle = 0. \quad (4.25)$$

For the supercritical bifurcation, which is the case with the normal Rayleigh–Bénard problem [2], we can find the steady amplitude of the convection cell from Eq. (4.25) as

$$\epsilon C_s = \sqrt{\frac{-(R-R_c)\left\langle \mathbf{y}, \boldsymbol{\beta}^{-1}\cdot\mathbf{G}^{(3)}\right\rangle}{\left\langle \mathbf{y}, \boldsymbol{\beta}^{-1}\cdot\mathbf{H}^{(3)}\right\rangle}}, \quad (4.26)$$

where Eq. (4.1) is invoked to replace R_2 in terms of R and R_c. From this, we can obtain the velocity and temperature field at the steady state for a given Rayleigh number if Eqs. (4.2) and (4.3) are exploited. Then, the Nusselt number Nu is given by

$$Nu = 1 - 2\left[(\epsilon C)_s\frac{\partial\Theta_1}{\partial y} + (\epsilon C)_s^2\frac{\partial\Theta_2}{\partial y}\right]_{y=-1}. \quad (4.27)$$

To corroborate the results of the nonlinear stability analysis, we solve the Boussinesq equation, Eqs. (2.20)–(2.22), using the Chebyshev pseudospectral method and compare the

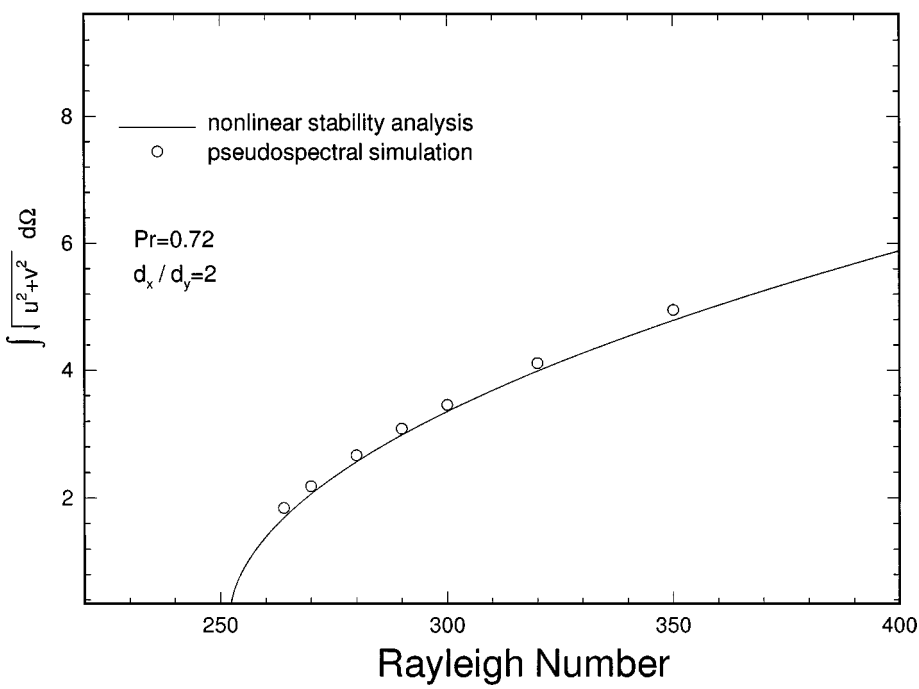

FIG. 8. Intensity of convection versus the Rayleigh number: comparison of the nonlinear stability analysis and the Chebyshev pseudospectral simulation when $Pr = 0.72$ and $d_x/d_y = 2$.

results with those of the nonlinear stability analysis. Details of the Chebyshev pseudospectral method as applied to the Boussinesq equation are given in Park and Chung [13]. Figures 7a and 7b plot the x-component, v_x (Fig. 7a), and the y-component, v_y (Fig. 7b), of the velocity vector, as obtained by the nonlinear stability analysis and the Chebyshev pseudospectral simulation, respectively, when $Pr = 0.72$, $d_x/d_y = 2.0$, the critical Rayleigh number $R_c = 251.8$, and the Rayleigh number $R = 300$. Figure 8 shows the intensity of convection, defined as the magnitude of the velocity integrated over the domain, versus the Rayleigh number when $d_x/d_y = 2.0$. The solid line denotes the convection intensity obtained by the nonlinear stability analysis, while that from the pseudospectral method is indicated by small circles. It is shown that the nonlinear stability analysis predicts correct convection

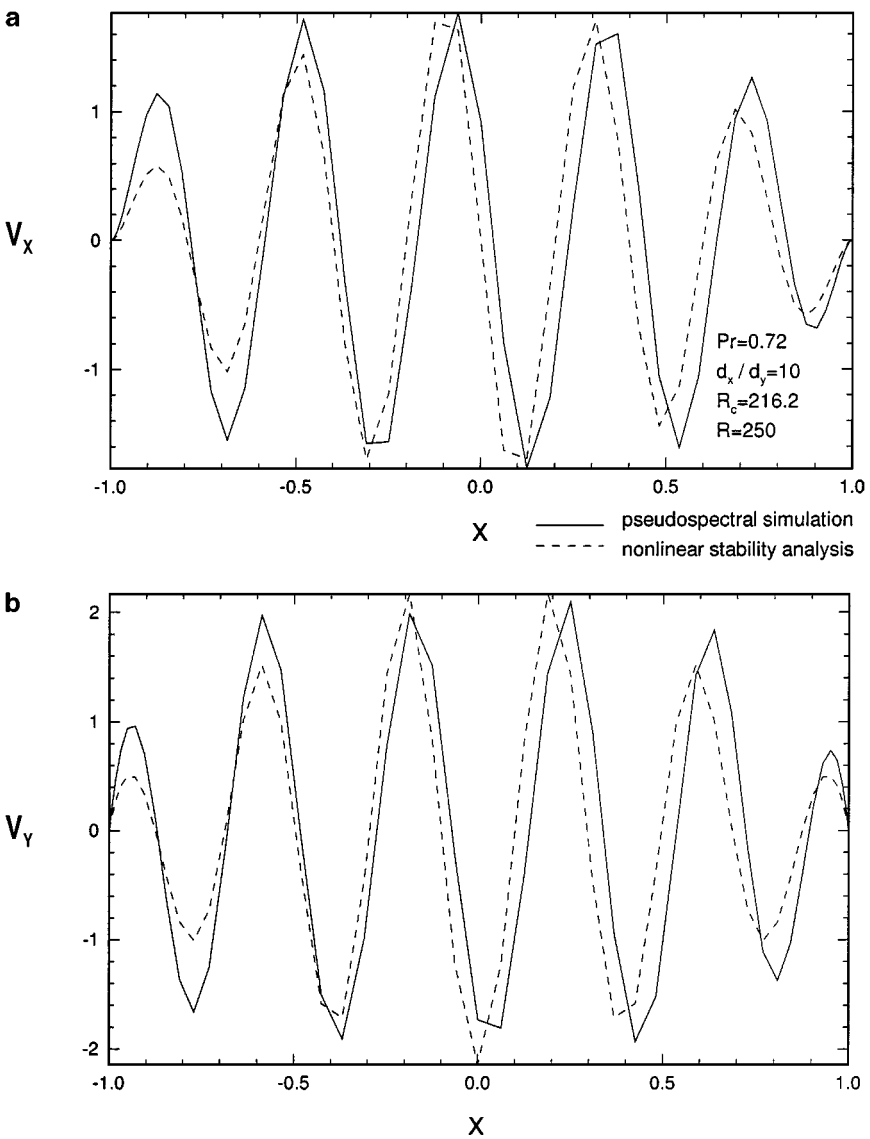

FIG. 9. Comparison of the nonlinear stability analysis with the Chebyshev pseudospectral simulation when $d_x/d_y = 10$, $R_c = 216.2$, and $R = 250$: (a) v_x, (b) v_y.

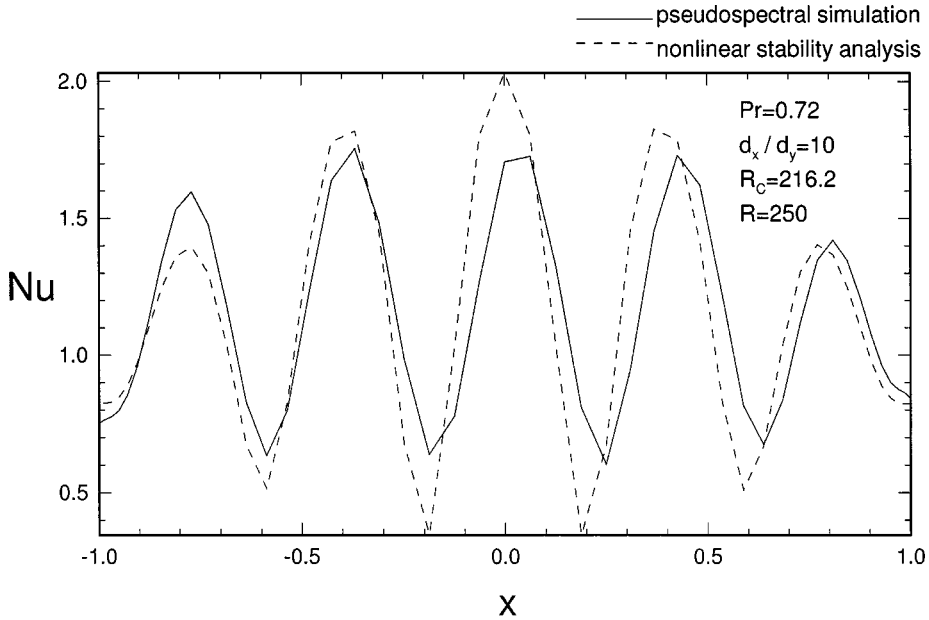

FIG. 10. Comparison of the Nusselt number when $d_x/d_y = 10$ and $R = 250$ ($R_c = 216.2$).

intensity even when the Rayleigh number R is over $1.5R_c$. Figures 9 and 10 show the comparison of velocity (Fig. 9) and Nusselt number (Fig. 10) obtained by the nonlinear stability analysis and pseudospectral simulation, respectively, when $Pr = 0.72$, $d_x/d_y = 10.0$, and $R = 250$. The critical Rayleigh number R_c is 216.2 when the aspect ratio d_x/d_y is 10.0. Figure 9a is for v_x, Fig. 9b is for v_y, and Fig. 10 is for the Nusselt number. Results from both the nonlinear stability analysis and the pseudospectral simulation show that the amplitude of convection cell diminishes near the sidewalls as a result of the nonslip boundary condition.

5. CONCLUSION

A method for performing linear and nonlinear hydrodynamic stability analysis in finite domains is developed. Specifically, in the present investigation, we consider a Rayleigh–Bénard problem in a two-dimensional domain where a heat source or a magnetic field that enhances or suppresses the convection may be present. By a judicious application of the Chebyshev pseudospectral method, the incompressibility condition is imposed exactly at the nonslip boundaries, avoiding the use of a penalty term that incurs numerical error. The present technique allows us to derive a Landau equation that predicts the evolution of the convection cell in a finite domain with respect to the Rayleigh number. The results based on the nonlinear stability analysis are compared with those obtained from the exact numerical solution of the Boussinesq equation, and both results are found to be in good agreement with each other. The present technique is quite versatile and may be employed to solve other hydrodynamic stability problems in finite domains. Although we consider two-dimensional problems in the present investigation, there are several avenues for extending the present technique to three-dimensional problems. If we assume the convection pattern in the three-dimensional domain to be poloidal [1], the present technique can be employed

without significant modification to solve the stability problem. Otherwise, we may employ the vector potential formulation or the primitive variables to solve more general three-dimensional hydrodynamic stability problems, both of which are methods currently being pursued.

REFERENCES

1. S. Chandrasekhar, *Hydrodynamic and Hydromagnetic Stability* (Oxford Univ. Press, London, 1961).
2. P. G. Drazin and W. H. Reid, *Hydrodynamic Stability* (Cambridge Univ. Press, Cambridge, UK, 1981).
3. W. V. R. Malkus and G. Veronis, Finite amplitude cellular convection, *J. Fluid Mech.* **4**, 225 (1958).
4. A. Schlüter, D. Lortz, and F. Busse, On the stability of steady finite amplitude convection, *J. Fluid Mech.* **23**, 129 (1965).
5. S. H. Davis, Convection in a box: Linear theory, *J. Fluid Mech.* **30**, 465 (1967).
6. B. D. Reddy and H. F. Voyé, Finite element analysis of the stability of fluid motions, *J. Comput. Phys.* **79**, 92 (1988).
7. A. I. van de Vooren and H. A. Dijkstra, A finite element stability analysis for the Marangoni problem in a rectangular container with rigid sidewalls, *Comput. Fluids* **17**, 467 (1989).
8. C. Canuto, M. Y. Hussaini, A. Quarteroni, and T. A. Zang, *Spectral Methods in Fluid Mechanics* (Springer-Verlag, Berlin, 1987).
9. D. Hatziavramidis and H. C. Ku, A pseudospectral method for the solution of the two-dimensional Navier–Stokes equations in the primitive variable formulation, *J. Comput. Phys.* **67**, 361 (1986).
10. H. M. Park and H. S. Lee, Nonlinear hydrodynamic stability of viscoelastic fluids heated from below, *J. Non-Newtonian Fluid Mech.* **60**, 1 (1995).
11. H. M. Park and H. S. Lee, Hopf bifurcations of viscoelastic fluids heated from below, *J. Non-Newtonian Fluid Mech.* **66**, 1 (1996).
12. A. Sterl, Numerical simulation of liquid metal MHD flow in rectangular ducts, *J. Fluid Mech.* **216**, 161 (1990).
13. H. M. Park and O. Y. Chung, Inverse natural convection problem of estimating wall heat flux, *Chem. Eng. Sci.* **55**, 2131 (2000).